

# An Evaluation of the Oxide Layers in Machining Swarfs to Improve Recycling

J. Uka, B. McKay, T. Minton, O. Adole, R. Lewis, S. J. Glanvill, L. Anguilano

**Abstract**—Effective heat treatment conditions to obtain maximum aluminium swarf recycling are investigated in this work. Aluminium swarf briquettes underwent treatments at different temperatures and cooling times to investigate the improvements obtained in the recovery of aluminium metal. The main issue for the recovery of the metal from swarfs is to overcome the constraints due to the oxide layers present in high concentration in the swarfs since they have a high surface area. Briquettes supplied by Renishaw were heat treated at 650, 700, 750, 800 and 850 °C for 1-hour and then cooled at 2.3, 3.5 and 5 °C/min. The resulting material was analysed using SEM EDX to observe the oxygen diffusion and aluminium coalescence at the boundary between adjacent swarfs. Preliminary results show that, swarf needs to be heat treated at a temperature of 850 °C and cooled down slowly at 2.3 °C/min to have thin and discontinuous alumina layers between the adjacent swarf and consequently allowing aluminium coalescence. This has the potential to save energy and provide maximum financial profit in preparation of swarf briquettes for recycling.

**Keywords**—Aluminium, swarf, oxide layers, recycle, reuse.

## I. INTRODUCTION

MANAGING swarf from production sites has been a problem that is addressed since the early stages of metal processing in industry due to the complications that come with it in the working area. Complications range from; generation of mass swarf that reduces efficiency in production, large amount of heat in the swarf making it unsafe to handle, significant amount of cooling lubricant contaminating the swarf and wasting the resources. Aluminium processing and manufacturing businesses produce this swarf in high volumes i.e. Toyota in 2010 produced 1,600 tonnes a month aluminium swarf which were transported offsite [1], while in the other hand Hubco Forgings supplies foundries with 400 tons of compacted swarf [2], [3]. The problem persists still nowadays even though some research has been performed to offer possible solution as shown from [4]. It is important to find an optimised methodology for the maximum re-use of the swarfs and to solve this problem the focus should be on the fundamental behaviour of the swarfs as they are treated for recycling. This paper aims to provide results on the bonding and coalescence between swarfs after heat treatment in different conditions.

J. Uka, B. McKay, T. Minton, O. Adole and L. Anguilano\* are with the Brunel University London, United Kingdom (\*corresponding author, e-mail: lorna.anguilano@brunel.ac.uk).

R. Lewis and S. J. Glanvill are with the Renishaw, Gloucestershire, United Kingdom.

This research did not receive any specific grant from funding agencies in the public, commercial, or not-for-profit sectors.

## A. Aluminium Oxide Layer

Alumina is the main barrier making it significantly difficult to recycle the swarf in solid billets using 100% swarf. As such it is important to study the behaviour of the swarf (alumina layer and aluminium) at high temperatures to find the optimal conditions to bring this material back to life without mixing it with virgin aluminium. In particular the fundamental behaviour of the aluminium/alumina interaction are the focus of this study to evaluate how to best break the alumina layers forming the external “crust” of each swarf within the briquette and impeding the coalescence of aluminium metal.

For this purpose, there are two experimental hypotheses: (1)- Aluminium trapped inside the alumina envelope is going to expand in volume with an approximate linear expansion  $24 \times 10^{-6} \text{ m/m}^\circ\text{C}$  [5] as the temperature increases and begin to melt, the forces generated by such expansion can support the breakage of the oxide layer. Fig. 1 shows thermal expansion coefficient for aluminium from different sources collected in one graph. This graph displays that aluminium thermal expansion increases as the temperature increases. When the temperature range is between 600-900 K corresponding to 327-627 °C the gradient of the curve is steeper showing a higher increase in thermal expansion of aluminium.

In the conditions of heat treatment, once temperature has reached the melting point of aluminium, the aluminium trapped inside the alumina is assumed to have melted, forming in this way a liquid mass inside the still solid alumina walls. These alumina walls can stand a certain pressure and after that alumina layer cracks and allows aluminium to sink towards the bottom of the vessel. As such there should be a point at which force due to thermal expansion of aluminium surpasses the force of alumina grains stuck together. As such, (2)- Alumina during heat treatment is going to change in different parts of polymorphs which are going to result in structural change and ease the cracking of the alumina walls of the swarf. When gamma alumina which forms at around 450 °C goes through few transformations to  $\delta$ ,  $\theta$  and finally  $\alpha$  as the temperature increases from 600 °C to 1000 °C, the volume of alumina decreases significantly forming cracks in the alumina layer. It should be this range of temperatures at which liquid aluminium can get through the alumina cracks and sink. So, to find a way to break the alumina layer, it is important to study polymorphs of aluminium oxides and conditions at which it forms. That information is then used to find the right conditions to treat aluminium swarf in order to recover the maximum aluminium. Therefore, in order to find out the properties of the alumina polymorphs, the coexistence/stability of aluminium and alumina was traced back in the literature. It

is reported [6] that alumina polymorphs exist at different temperatures. The behaviour of these polymorphs at different temperatures gives a link to the way aluminium swarf needs to be treated to recover the aluminium from there. In Fig. 2 the forms of alumina and the temperature at which each polymorph exists are presented. The alumina phase depends on the material it initially originated from. The alumina, in the case of swarf derives from the oxidation of aluminium during machining and further oxidation which happens in the molten state of aluminium during the experiments, as such in Fig. 2 alumina coming from melt or amorphous phase is referred in the investigation (as highlighted in Fig. 2).

It is known that amorphous alumina forms on the surface of aluminium from the moment at which aluminium is produced. The thickness of layers formed by each phase changes and depends from the heat treatment temperature and the length of time at which the swarf is exposed at a certain temperature.

Reference [7] studied this in aluminium powder which is shown in Fig. 3. It can be observed that the thickness of each polymorph at different stages in aluminium powder is different [7]. The same happens with the mass of alumina which increases as the temperature increases and that can be referred to the fact that  $\alpha$  – alumina occupies smaller volume than  $\gamma$  – alumina. During the transformation new aluminium will get exposed to the environment and then oxidised, increasing in this way the alumina mass, as stated also from [8].

Reference [9] used a dilatometer to show that alumina layer shrinks as it transforms from  $\gamma$  to  $\delta$  and or  $\theta$  and then  $\alpha$ , exposing new aluminium to oxidation. As result the alumina mass increases. Fig. 4 shows the changes that alumina layer experiences with the temperature specifically the shrinkage starts at 1000 °C and increases very rapidly after 1200 °C.

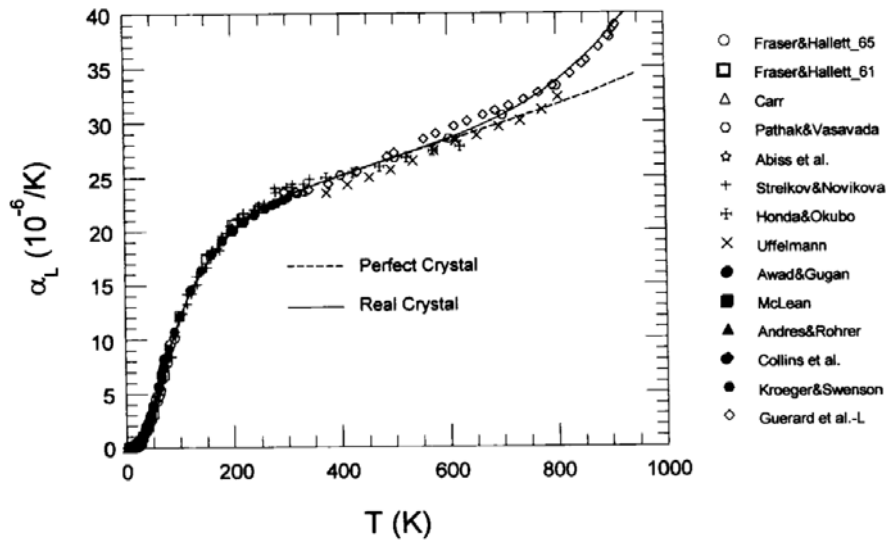


Fig. 1 The coefficient of thermal expansion for Al. The sources of the data are indicated by the symbols. The broken curve indicates the perfect crystal model and the solid curve represents the calculated real crystal model from [5]

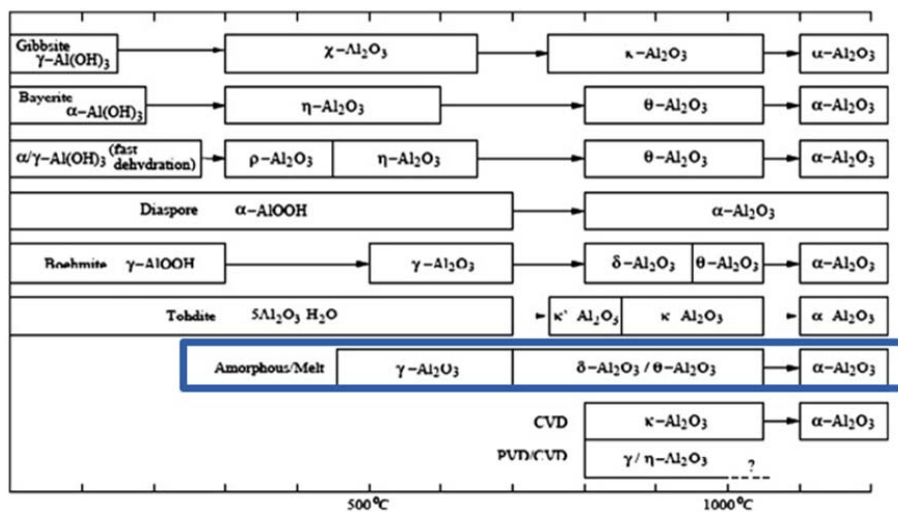


Fig. 2 Transition sequences of alumina starting from forms of aluminium hydroxide or amorphous alumina / melt [6], highlighted in the blue rectangle in the figure

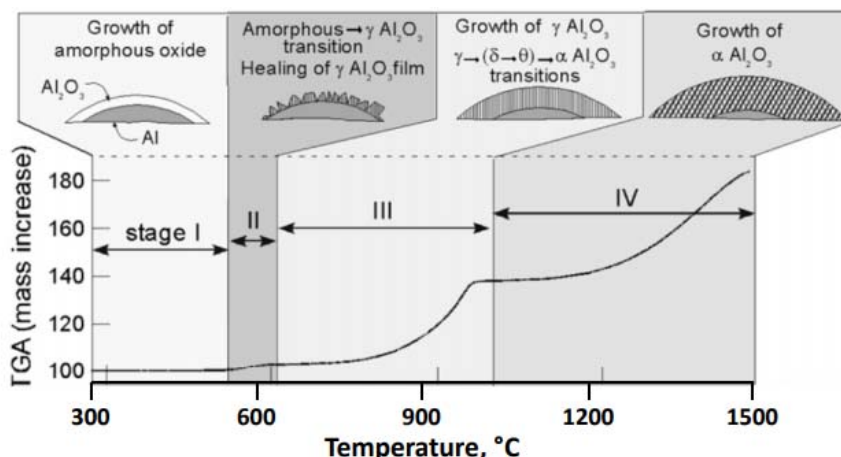


Fig. 3 Schematic representation of transitions occurring in alumina layer on aluminium metal, and the temperature ranges in which they occur, superimposed on a typical TGA plot [7]

$\gamma$ -alumina transforms in  $\alpha$ -alumina which has a smaller volume. Based on XRD calculation, it is shown by the Scherrer equation that while  $\alpha$  alumina has a crystallite shape of about 33 nm, the  $\gamma$  alumina lies within the range of 5.0-10.0 nm [10]. This process of atoms rearranging to form a smaller volume structure results in cracks in the oxide layer. When this happens oxygen can penetrate and oxidise more aluminium from the layer exposed as such it will increase the rate of oxidation. This is the point where environment needs to be controlled. Additionally, the rate of oxidation can be affected from certain factors such as:

- Humid air in the beginning increases the oxidation of aluminium melt after that phase oxidation decreases and can be maintained at that rate for about 72h [11], [12].
- The addition of nitrogen ( $N_2$ ) to the oxygen atmosphere prolongs the period of slow oxidation before the onset of breakaway oxidation.
- Argon (Ar) has a similar effect of slowing oxidation, but the effects are not as pronounced when used in similar quantities (typically 4 parts to 1 of air).
- Carbon dioxide ( $CO_2$ ) also slows the onset of breakaway oxidation. It has been shown that when 65%  $CO_2$  atmosphere (air balance) is used, breakaway oxidation can be halted for around 16-18 hours, but with 50%  $CO_2$  or less it occurs after around 1 hour.
- Flue gas containing water vapour,  $N_2$  and  $CO_2$  was also found to slow oxidation, although it did not have as strong an effect as  $CO_2$  alone.

If aluminium gets exposed to higher temperatures then the oxide layer thickness increases, additionally the temperature affects the uniformity of the oxide layer. At lower temperature the oxide layer is uniformly spread and in amorphous phase, at higher temperatures such as 400 °C and above amorphous layer starts to convert into crystalline form of  $Al_2O_3$  [13].

Alloying elements' additions and impurities affect the oxidation rate in different ways. Magnesium and copper for instance increase the oxidation rate of aluminium while beryllium reduces it. Campbell 2015 states that alkali metals could cause the alumina to reduce back to aluminium as they

form a stable oxide. On the contrary, [15], reported that elements such as sodium, calcium and selenium have been shown to increase the oxidation rate of pure aluminium, whilst a presence of boron or titanium can result in a thicker oxide. Silicon is reported to have no effect in the oxidation rate while copper and zinc increase it with the difference that zinc increases the incubation period before the breakaway oxidation as it happens with copper.

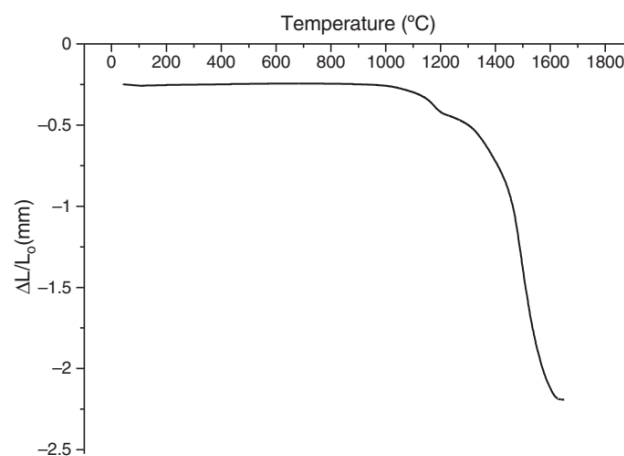


Fig. 4 Dilatometry curve of the  $\gamma$ - $Al_2O_3$  transition alumina sample heated up to 1700 °C at 5 heating rates [9]

Time of exposure of aluminium to a certain temperature and the alloying elements together affect the aluminium oxide layer. As the time of exposure in high temperature increases the oxide layer surrounding the aluminium increases in thickness, however after the layer reaches certain thickness then it is not going to change parameters for some time up to 8 hours [16].

All this information indicates that temperatures at which the recovery of aluminium needs to be performed at the range where  $\gamma$ -alumina starts to transform into  $\delta$  or  $\theta$  and the best is as it transforms to  $\alpha$ -alumina as at this point a significant decrease in volume of alumina is observed. This range of temperatures is 700 °C to 1100 °C. All this information is true

for pure aluminium however in the study presented here is used swarf from a mixture of 6000 series aluminium alloys. Additional elements contained by the alloys could affect the behaviour of swarf during heat treatment, thus heat treatment analysis would clarify important steps to take during heat treatment of swarf to recover aluminium.

## II. METHODOLOGY

During this work aluminium swarf briquetted from the machining processes at Renishaw were received and analysed for its composition. Then this material was heat treated at different temperatures to analyse the behaviour of the swarf with these conditions. As such the work itself was divided in 5 stages:

1. Compositional analysis of material as received;
2. Heat treatment of the briquettes at conditions pre-defined in the Design of Experiment (step 3);
3. Section, mount, grind and polish heat treated briquettes for SEM analysis;
4. Perform SEM elemental mapping for all the samples;
5. Analyse the data collected.

### A. Step 1 – Analysing the Composition of Aluminium Swarf

Mixed aluminium machining swarf was received from Renishaw in the form of briquettes with a dimension approximately  $\phi = 100$  mm and  $l = 120$  mm as shown in Fig. 5.



Fig. 5 As received briquette from Renishaw.

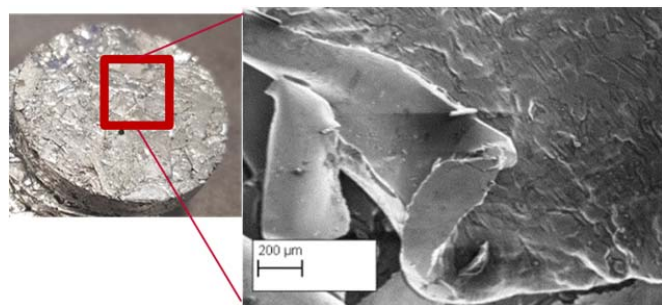


Fig. 6 A pellet and one SEM image from that pellet

From each briquette 5-10 grams of swarf has been removed from both sides of the briquette. Loose swarf then is mixed and pelletised using hydraulic press. In this way the material received was assumed to be a comprehensive representation of the overall briquette. The pellet, with diameter  $\phi = 40$  mm,

was used to analyse the chemical composition of the swarf.

TABLE I  
COMPOSITION OF SWARF

Weight % for 30 briquettes		
Element	Average	Range
Al	93.2	86.8 - 96.5
O	2.4	0.3 - 5.2
Mg	1.6	0.6 - 5.3
Mn	0.5	0.3 - 2.2
Si	2.0	0.4 - 5.8
Fe	0.3	0.1 - 1.5

The prepared samples undergo the elemental analysis using SEM-EDS. The analysis was performed using Zeiss LEO equipped with an energy dispersive spectrometer EDAX Octane Superior An energy of 20 kV and 300 mA current was used. Analyses were performed on three subsurfaces of approximately 2 mm<sup>2</sup>. Then an average of the composition was calculated. The same procedure was repeated for 30 pellets taken from 30 different briquettes. Then an overall average was calculated and presented as the composition of the swarf in Table I. From the elemental analysis performed it appears that this swarf is more similar to 6082 aluminium alloy.

### B. Step 2 Briquettes Heat Treatment Experiment

The remaining of the briquette with a mass between 350-450 g would be placed in a silicon-carbide graphite crucible with diameter  $\phi = 128$  mm and height 145 mm. The crucible was then placed in an electric resistance furnace (Carbolite) and heat treated using the following conditions:

- Temperatures 650, 700, 750, 800, 850 °C.
- Three briquettes were heat treated at each temperature; however, they were cooled with different cooling rates: 2.5, 3.5 and 5 °C/min.
- These series of experiments were repeated for heat treatment times 1 h.

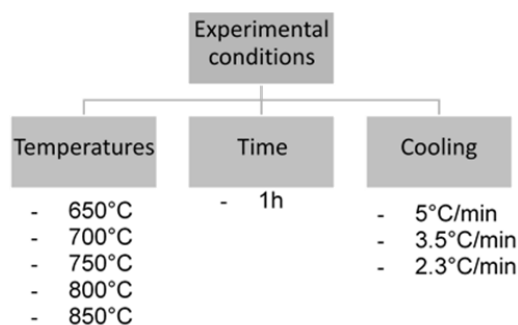


Fig. 7 Experimental conditions

In Fig. 7 the experimental conditions are shown at which the aluminium alloy 6082 swarf briquettes have undergone before analysing the results.

### C. Step 3 Sample Preparation for SEM Analysis

Heat treated briquettes were sectioned as shown in Fig. 8 to obtain three sub-samples from the core of the solidified

sample in order to observe the distribution of the oxides throughout the length of the briquette. This was done by proxy evaluating the distribution of oxygen in the sample using chemical mapping in three areas of the sample: top, middle and bottom. The method assumes that wherever oxygen was detected that oxygen is bonded with aluminium and not any

other element present. In reality, the weight percentage (%wt) of other elements in this swarf is very small, as can be noted in Table I. The samples that display the least amount of oxygen in the mapping indicate the more optimal conditions to overcome the barriers of alumina distancing between aluminium grains.

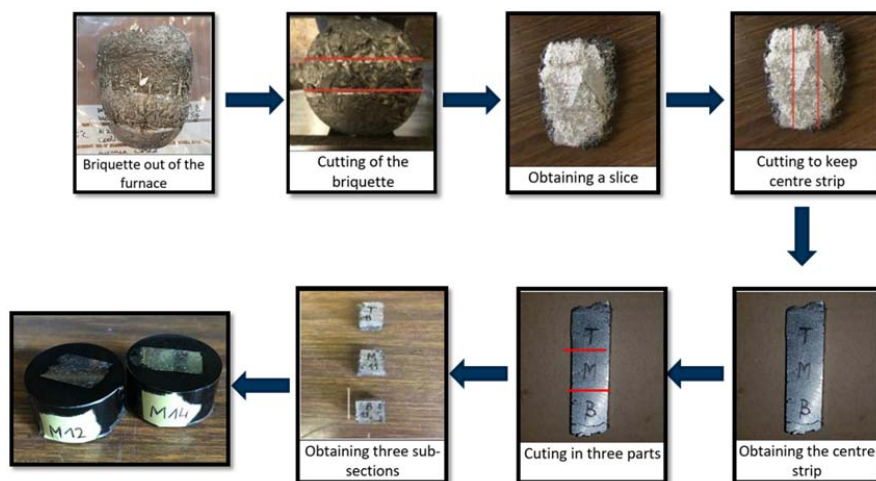


Fig. 8 Steps to prepare the sub-samples from the briquette for SEM analysis

The samples were mounted in conductive resin at 180 °C under pressure 200 Pa and then ground using four different silicon carbide grinding papers with mesh 600, 1200, 2500 and 4000. For this purpose, an automated grinding machine with 160 rpm head rotation and 20 rpm base rotation was used.

#### D. Step 4 - Perform SEM Elemental Mapping for All the Samples

Samples then were observed in the SEM using Zeiss Supra 35VP with energy 20 kV equipped with EDAX Octane Superior EDS system to identify the oxide layer and evaluate the conditions at which the relative wt% of oxygen in the sample is the lowest. It is important to note that the magnification for all SEM samples is comparable and the analysed area is approximately 2.25 mm<sup>2</sup>. The reason for using low magnification is to observe the continuity of alumina layers, relative oxygen concentration and its thickness.

### III. RESULTS

This analysis consists of comparing the relative (%wt) oxygen in the samples of aluminium swarf which has been treated at different temperatures for one hour in the furnace at three different cooling rates. EDS elemental mapping provides further information on the oxygen distribution and the thickness of oxygen layers throughout the length of the briquette. Analysing all this information informs of the conditions at which the oxide layer is the thinnest and/or discontinuous and as such facilitates a maximum yield of the aluminium from swarf.

#### A. Distribution of the Oxygen throughout the Length of the Briquette

Three types of data were obtained from EDS elemental mapping; relative %wt of oxygen, oxygen distribution throughout the length of the briquette and relative thickness of oxide layers. For purpose of the analysis it is assumed that oxygen allocated in the sample is bonded with aluminium to form alumina.

TABLE II  
RELATIVE %WT OF OXYGEN RESPECTIVELY AT THE BOTTOM (B), MIDDLE (M) AND TOP (T) OF THE BRIQUETTE DEPENDING ON THE COOLING RATE AND TEMPERATURE OF HEAT TREATMENT

Heat Treatment Temperature (°C)	Cooling rate (°C/min)	Briquette Sections		
		B	M	T
650	5	14	5	7
	3.5	8	12	25
	2.3	14	14	22
700	5	8	6	
	3.5	5	9	9
	2.3	13	9	12
750	5	5	6	10
	3.5	5	10	12
	2.3	9	5	17
800	5	3	5	7
	3.5	5	5	5
	2.3	1	3	15
850	5	1	4	4
	3.5	1	3	5
	2.3	9	5	43

Preliminary data have shown that the relative %wt of oxygen changes according to heat treatment conditions. In

Table II the relative %wt of oxygen are shown for three parts of the briquette heat treated in the given temperatures. From Fig. 9 in the bar chart it can be observed that the relative %wt of oxygen decreases as the heat treatment temperature increases in the briquette.

All the briquettes that have cooled down at a rate of 2.3 °C/min have displayed lower %wt of oxygen compared with briquettes treated at the same temperature but cooled down at a quicker rate. This pattern seems to appear different if we compare the bottom and middle of briquettes for the same heat treatment temperature but at different cooling rates. It is observed that in any case the %wt distribution in the middle of the briquette is lower during 2.3 °C/min compared with 3.5 °C/min and sometimes even lower than %wt of oxides in the middle of the briquette for 5 °C/min cooling rate as in the case of heat treating the briquette at 750 °C. Briquettes are heat treated at 650 °C and cooled down quickly 2.3°C/min has the highest average content of %wt oxygen. It can be observed that for each temperature the overall %wt of oxygen increases as the cooling rate increases. The heat treatment temperature which gives the lowest relative %wt of oxygen in any of the parts of the briquette is 850°C, cooling down at 2.3 °C/min. Another interesting part of this experiment is the case that at 850 °C for cooling rate of 2.3 °C/min there appears a drastic increase in relative weight % of oxygen, the level of oxidation in this briquette could have been due to unprecedented levels of contaminations such as cooling/lubricant oil or other wastes that could have joined the swarf during briquetting process as such that is considered an outlier.

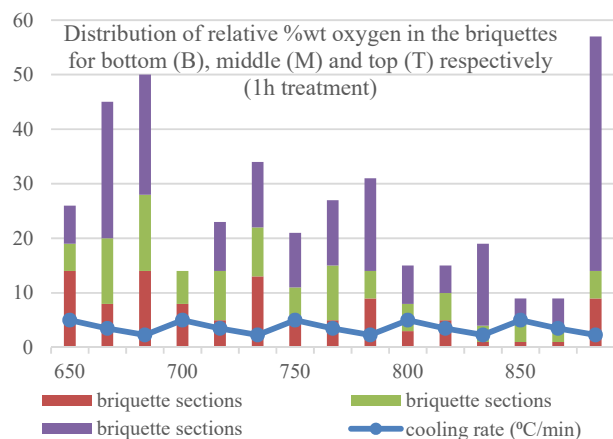


Fig. 9 Distribution of relative %wt oxygen in three different parts of the heat treated briquettes (bottom, middle, top) at 650, 700, 750 800 850 °C for three different cooling rates respectively at 5 °C/min, 3.5 °C/min and 2.3 °C/min

Next step is to observe the EDS elemental mapping for oxygen for the samples for temperatures 60, 70, 75, 800 and 850 °C with cooling rate as shown in Table II. The EDS elemental mapping shown in Table II indicates that relative oxygen varies from 5wt%-25wt%, with 12 areas out of 27 displaying a wt% of oxygen above 10%. The oxide layers are as thick as 450µm in some case and continuous throughout the surface which shows that aluminium was not able to break the

alumina layer surrounding it. However, for temperatures 800 °C and 850 °C it can be clearly observed that percentage weight of the oxides falls to 1%, the thickness of the layers is 63-126 µm. The layers appear discontinuous and some alumina is gathered in a lump shape in certain areas. The gaps can be as large as 300 µm in the sample treated at 850 °C in the bottom part of the briquette.

Next step is to identify how the weight percentage of oxides changes throughout the length of each briquette. Observing the data for 3 parts of briquette throughout all 15 briquettes available on the table, it can be stated that oxides are less concentrated at the bottom of the briquette. However, they are heavily concentrated, in as much as 6 layers of oxides for 500 µm linearly, at the top of the briquette. Exception to this has made 31-C and 32 – O shown in Table III which has a bottom part of the briquette packed with oxide layers. These data show that molten aluminium sinks at the bottom of the briquette if it will find a discontinuity in the swarf flakes leaving behind at the top of the briquette some aluminium locked into thick oxide layers, furthermore some more aluminium gets oxidised because hot aluminium is in contact with air. Oxide layers in this region get concentrated and press upon one another.

Another pattern about oxide distribution is observed in the perspective of cooling rates. Every time in the experiments the briquettes cooled fast, the oxide layers distributed more uniformly throughout the briquette such as briquette 21-O. The sample shows more oxides in terms of percentage weight and the layers are continuous and thick. To illustrate this case a reference to briquette number 33, 28 and 23 is made which is shown in Table IV.

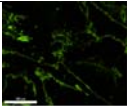
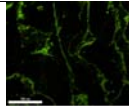
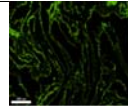
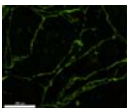
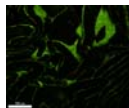
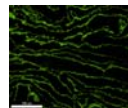
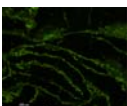
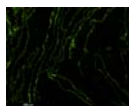

TABLE III  
WEIGHT PERCENTAGE DISTRIBUTION OF OXYGEN IN THE BRIQUETTES HEAT TREATED FOR 1 HOUR AT SELECTED EXPERIMENTS COOLED AT THREE DIFFERENT RATES

Temperature (°C)	Briquette number	Bottom	Middle	Top	
650	21 – 2.3 °C/min				
		Oxide thickness (µm)	20 - 150	20 - 350	20 - 400
		Gaps (µm)	continuous	continuous	continuous
		Relative oxygen	14%	14%	22%
750	32 – 2.5 °C/min				
		Oxide thickness (µm)	20 - 250	20 - 60	20 - 100
		Gaps (µm)	continuous	continuous	continuous
		Relative oxygen	13%	9%	12%
850	35 – 5 °C/min				
		Oxide thickness (µm)	10 - 40	10 - 80	10 - 60
		Gaps (µm)	60 - 100	40 - 100	continuous
		Relative oxygen	1%	4%	4%

Briquette 33 cooled down at 2.5 °C/min has been

characterised with a concentration of oxides of 5 %wt for the bottom of the briquette, 6 %wt for the middle part of the briquette and 10 %wt for the top of the briquette. Briquette number 28 cooled down at 3.5 °C/min and percentage weight of oxides is as follows: 5%,10%, 12% respectively for bottom, middle and top. And briquette number 23 which is cooled down at 5 °C/min contains a weight distribution of oxides 9%, 5% and 17% in the same sections. The same trend is observable throughout all the performed experiments. This shows that if the sample will be left to cool down slowly the weight percentage of oxides decreases in the bottom section because the liquid aluminium can sink through the gaps of alumina and sink down in the bottom part of the crucible.

TABLE IV  
WEIGHT PERCENTAGE DISTRIBUTION OF OXYGEN CONSIDERING COOLING RATE EFFECT

Temperature (°C)	Briquette number	Bottom	Middle	Top
750	33 - 5°C/min			
Oxide thickness in (µm)		20 – 200	20 - 100	10 - 120
Gaps (µm)		continuous	continuous	continuous
Relative oxygen		5%	6%	10%
28 – 3.5 °C/min	28 - 3.5 °C/min			
Oxide thickness in (µm)		10 -70	10 -300	20-80
Gaps (µm)		30	15	continuous
Relative oxygen		5%	10%	12%
23 – 2.5 °C/min	23 - 2.5 °C/min			
Oxide thickness in (µm)		30 -100	10 – 60	10 - 150
Gaps (µm)		continuous	continuous	continuous
Relative oxygen		9%	5%	17%

From the data collected until now results that the best conditions where minimum oxides are observed and maximum aluminium is recovered are to treat aluminium for one hour at 850 °C and cool the briquette at 2.5 °C/min. The relative oxygen content is around 1% and the oxide layers are discontinuous, while their thickness varies from as low as 15 µm in the sample taken from the bottom of the briquette to 150 µm for the bottom of the briquette.

#### IV. DISCUSSION

The results showed that the %wt of oxygen decreased as the heat treatment temperature increased in the briquette. This could happen due to oxygen mixing well with the matrix of aluminium as the heat treatment occurs or due to the temperature gradient between aluminium alloy and in the swarf flake. The second one is due to the time needed for temperature to travel from the surface of the flake where aluminium oxide layer lies and the inner part of the flake

where aluminium alloy is found. In higher temperature the equilibrium temperature is reached quicker giving less time for oxygen to travel inwards and oxidise the rest of aluminium in the swarf before it liquefies and starts to move around. Once the aluminium alloy has liquefied, the oxygen from the swarf could travel towards the inner part due to the turbulence in the melt. In this way any new alumina particles formed get distributed and scattered within the liquid alloy

The effect of thermal expansion of aluminium inside the swarf it is high up to the point when the aluminium melts. During that time the spacing between atoms increases which results in some force applied in outwards direction in the alumina walls around the swarf. Once aluminium is liquid then atoms are in the movement and adjust themselves to fit within the room it is given to them, furthermore the volume of liquid even could decrease due to particles fitting in the gaps between atoms that used to be in the lattice as described by [15].

Observing the behaviour of the oxides in 3 different cooling rates and showing that the fast cooling rate results in high content %wt of oxygen shows that in the case of faster cooling rate could be that there is not sufficient time for the molten aluminium to circulate, coalesce and sink down in the crucible.

In the EDS mapping for temperature treatment 650, 700, 750, 800 and 850 has shown that heat treatment at 800 and 850 degrees the alumina layers are thinner and they show gaps throughout the areas where the boundary of swarf flake was meant to be. During the process of the melt as aluminium is liquefied in the flake is expanding pushing the walls of the alumina layers, in the other hand alumina starts to transform from  $\gamma \rightarrow \delta/\theta \rightarrow \alpha$ . First transformation  $\gamma \rightarrow \delta/\theta$  occurs at just under 700. For this reason, for the briquettes heat treated at 650 °C liquid aluminium during its thermal expansion cannot break throughout the wall or react with it due to this very strong amorphous layer of alumina, for this reason the alumina layers appear thick and continuous. As the temperature increases and the transformation of alumina from  $\gamma \rightarrow \delta/\theta$  occurs more gaps in the alumina layer are observed. It is well known that as this phase transformation of alumina occur the volume that the alumina occupies decreases providing gaps for the liquid aluminium to escape from alumina envelope. As such the temperatures where more gaps were visible during heat treatment were at 800 and 850. This also is because the higher the temperature the more phase transformation has occurred and carries on towards transformation from  $\delta/\theta \rightarrow \alpha$ .

Observation of relative %wt of oxygen distributed throughout the briquette changes due to gravity. Once the aluminium alloy has been able to escape the alumina envelope it sinks down in the crucible making the lower part of the briquette to have less relative %wt of oxygen and the middle has an intermediate amount because not all of aluminium have managed to escape properly or it has solidified before going to the bottom of the briquette and the top of the briquette has the highest amount of relative %wt oxygen. This was confirmed with the briquettes that were cooled down in three different cooling rates. Briquettes cooled down 5 °C/min had always the

most amount of aluminium alloy gathered at the bottom of the briquette with the least amount of oxides in this area. Finding an effective way to break these oxides inside the aluminium alloy matrix and uniformly distribute or even orientate them in the matrix would result in the production of valuable advanced composites.

#### V. CONCLUSIONS

This study focusses on oxide behaviour of swarf in the melting temperatures of aluminium in order to provide an assessment on how to recycle 100% swarf briquettes for the potential re-use of swarfs directly in the manufacturing plants.

During this work it has been observed that:

- As the temperature increases less oxides will be found in the briquette in the form of thick continuous layers.
- Throughout the briquette for temperatures above 750 °C the aluminium starts to sink at the bottom of crucible and oxides are concentrated at the top of briquette.
- Thermal expansion is significant only during the first stage until the aluminium inside the alumina walls in swarf melts, after that the impact is going to be insignificant or it even could be negative.
- Slow cooling rates give enough time for aluminium to sink in the crucible particularly because no cold fresh air is introduced around the briquette and the high temperatures give enough time to aluminium to find discontinuity in the oxide layer and then sink down.
- The best condition to treat aluminium swarf until now to retrieve aluminium are to keep the briquette in the furnace for one hour at 850 °C and cool it down at 2.5 °C/min.

#### REFERENCES

- [1] Toyota, "Toyota Resource Efficiency," ed, 2021.
- [2] F. Planet, "Foundry planet," ed: Hubco Forgings, 2010.
- [3] P. Foundry, "Planet Foundry," ed: Hubco Forgings, 2010.
- [4] Uka J, McKay B, Minton T, Lewis R and Anguilano L\*, "Methods to Re-Use and Recycle Aluminium," *Evolutions in Mechanical Engineering*, vol. 3, no. 2, p. 4, 2020.
- [5] K. Wang and R. R. Reeber, "The perfect crystal, thermal vacancies and the thermal expansion coefficient of aluminium," *Philosophical Magazine A*, vol. 80, no. 7, pp. 1629-1643, 2000, doi: 10.1080/01418610008212140.
- [6] Y. L. Wu, J. Hong, D. Peterson, J. Zhou, T. S. Cho, and D. N. Ruzic, "Deposition of aluminum oxide by evaporative coating at atmospheric pressure (ECAP)," *Surface & Coatings Technology*, vol. 237, pp. 369-378, 2013, doi: 10.1016/j.surfcoat.2013.06.043.
- [7] M. A. Trunov, M. Schoenitz, and E. L. Dreizin, "Effect of polymorphic phase transformations in alumina layer on ignition of aluminium particles," *Combustion Theory and Modelling*, vol. 10, no. 4, pp. 603-623, 2006, doi: 10.1080/13647830600578506.
- [8] J. M. Campbell, *Castings*, 2nd ed. (no. Book, Whole). Oxford; Boston; - eBook: Butterworth-Heinemann, 2003.
- [9] S. Lamouri *et al.*, "Control of the  $\gamma$ -alumina to  $\alpha$ -alumina phase transformation for an optimized alumina densification," *Boletín de la Sociedad Española de Cerámica y Vidrio*, vol. 56, no. 2, pp. 47-54, 2017/03/01/ 2017, doi: <https://doi.org/10.1016/j.bsecv.2016.10.001>.
- [10] Nanografi, "Differences between Alpha and Gamma Alumina nanoparticles," in *Blografi* vol. 2020, ed. <https://nanografi.com/blog/differences-between-alpha-and-gamma-alumina-nanoparticles/>, 16 Sep 2019.
- [11] S. A. Impney, D. J. Stephenson, and J. R. Nicholls, "Mechanism of scale growth on liquid aluminium," *Materials Science and Technology*, vol. 4, no. 12, pp. 1126-1132, 1988/12/01 1988, doi: 10.1179/mst.1988.4.12.1126.
- [12] P. E. Blackburn and E. A. Gulbransen, "Aluminum Reactions with Water Vapor, Dry Oxygen, Moist Oxygen, and Moist Hydrogen between 500° and 625°C," *Journal of The Electrochemical Society*, vol. 107, no. 12, p. 944, 1960, doi: 10.1149/1.2427576.
- [13] L. P. H. Jeurgens, W. G. Sloof, F. D. Tichelaar, and E. J. Mittemeijer, "Composition and chemical state of the ions of aluminium-oxide films formed by thermal oxidation of aluminium," *Surface Science*, vol. 506, no. 3, pp. 313-332, 2002, doi: 10.1016/S0039-6028(02)01432-2.
- [14] G. M. Scamans and E. P. Butler, "In situ observations of crystalline oxide formation during aluminum and aluminum alloy oxidation," *Metallurgical Transactions A*, vol. 6, no. 11, pp. 2055-2063, 1975/11/01 1975, doi: 10.1007/BF03161831.
- [15] M. Drouzy and C. Mascré, "The oxidation of liquid non-ferrous metals in air or oxygen," *Metallurgical Reviews*, vol. 14, no. 1, pp. 25-46, 1969/01/01 1969, doi: 10.1179/mtr.1969.14.1.25.
- [16] E. M. Hinton, "The oxidation of liquid aluminium and the potential for oxides in grain refinement of aluminium alloys," University of Birmingham - Dissertation, Dissertation/Thesis, 2016. (Online).